



M Ű E G Y E T E M 1 7 8 2

Budapest University of Technology and Economics
Faculty of Electrical Engineering and Informatics
Department of Info-communication and Electromagnetic Theory

Investigation of Potential 5G Modulation Formats in mm-wave Radio over Fiber
Systems and Passive Optical Network

Ph.D. Thesis booklet

Hum Nath Parajuli
M.Sc., Electronics Engineer

Supervisor:
Dr. Eszter Udvary Gerhátné

Budapest, 2018

1. Introduction

In recent years, the demand of huge amount of bandwidth is rapidly growing due to the growing use of bandwidth demanding devices and applications such as smart phones, streaming of video, cloud computing, video games etc. The limited wireless bandwidth at conventional radio frequency (RF) bands (0.7-2.6 GHz) is not sufficient to fulfill these demands [1]. Future wireless 5G networks are expected to provide 1-10 Gbps wireless access to the end users [1-5]. The major approaches to resolve the problem of bandwidth/data rate demand can be put as: a) frequency reuse through small cell deployment, b) use of higher frequency bands such as millimeter wave (mm-wave) bands and c) spectral efficiency improvement using advanced modulation formats and multiplexing techniques. All these approaches can be effectively realized with the help of radio over fiber (RoF) technology. In RoF technology, the wireless signal is transmitted into remote cells with optical means. By reducing the cell size, frequency reuse can be done more repeatedly. Higher frequency bands such as mm-wave bands can provide Gbps wireless access however it suffers from huge path loss resulting limited transmission range. Therefore, small cells architecture in combination with mm-wave RoF provides a superior solution to increase the cellular system capacity. The advanced modulation formats and multiplexing technologies offer the suitable spectral efficiency to provide the needed capacity for the end users. Thus, to provide Gbps wireless access to the end users, the RoF technologies with mm-wave bands and utilization of advanced modulation schemes will be extremely important.

The modulation signal in RoF is an RF and thus the data is modulated with sideband scheme. Three major sideband schemes used in RoF systems are optical double sideband (ODSB), optical single sideband (OSSB) and optical carrier suppressed double sideband (OCS-DSB) schemes. These schemes can be achieved with both intensity modulation and angle modulation of the optical carrier. The optical sideband modulation method plays important role in maintaining the better system performance. ODSB and OSSB schemes can deliver the vector signal to the receiver. However, ODSB is seriously affected by chromatic dispersion (CD) which leads to the power fading of the received signal and not suitable for long reach and high-frequency RoF system if constant power gain is required. OCS-DSB scheme can compensate the CD and provides the best signal to noise ratio (SNR). However, this scheme cannot be used for vector signal transmission without doubling the signal frequency and phase at the receiver, as a consequence the sent signal will be modified while detecting at the receiver [6]. OSSB can compensate the CD but requires a more complex method for its generation and suffers from serious SNR degradation due to the strong dc component present in the detected signal. Since CD is the major transmission fiber impairment in RoF system, OSSB scheme is a common choice in RoF system due to the need of compensating CD [7-9]. In this thesis, I theoretically and experimentally demonstrated the technique for SNR improvement in OSSB

using unequal sideband intensity based modulation scheme called optical vestigial sideband modulation scheme (OVSB). With this method, the system performance can be improved by enhancing the SNR as well as maintaining the CD compensation.

Higher frequency bands such as mm-wave bands are considered as a solution to overcome the problem of frequency congestion in current wireless transmission systems [2-5]. Due to the huge path loss in higher frequency bands, there will be the need for deployment of a large number of small cells; thus complex base station (BS) transceiver is not cost effective. Therefore, simple modulation method and detection method is required. In this thesis, I experimentally realized the mm-wave RoF system with advanced modulation formats using direct detection method. 4G LTE or LTE-A is used for the mobile broadband (MBB) application which is based on the cyclic prefix orthogonal frequency division multiplexing (CP-OFDM) modulation. However, the drawbacks of the CP-OFDM are spectral inefficiency and large out of band emission (OOB). The alternative multicarrier modulation schemes are considered as a potential solution to overcome the problem of spectral inefficiency for future generation wireless systems. In this context, the potential 5G modulation formats such as filter bank multi-carrier (FBMC), universal filter multi-carrier (UF-OFDM) have to be explored more and more to achieve the commercial realization in the near future. FBMC and UF-OFDM modulation formats are considered as potential candidates for future wireless 5G. In this thesis, I experimentally evaluated the performance of these modulation formats in mm-wave RoF environment.

The passive optical network (PON) provides the high capacity and flexibility in signal delivery through the fixed access network. PON is considered as an effective solution for 5G based wireless signals backhauling and fronthauling [10-15]. The future 5G systems should be capable of supporting multi-services/signals to keep the compatibility with the current legacy wired/wireless services. In this regard, it is important to study and analyze the convergence and delivery of potential 5G wireless signals with wired signals in the future PON systems. In this thesis, I experimentally evaluated the convergence performance of wired 4-pulse amplitude modulation (4-PAM) and wireless potential 5G modulation formats (UF-OFDM, FBMC) signals in PON.

2. Investigation methods

The major objective of this research is to evaluate experimentally potential 5G modulation formats in the RoF systems. To verify the principle of the OVSB, the experimental as well as numerical simulations have been performed. Also, to analyze the performance of the potential 5G modulation formats in mm-wave RoF system as well as in the PON, I designed and studied numerical simulation setup as well as experimental setup.

VPItransmissionMaker simulator along with MATLAB co-simulation is used to implement and evaluate the performance with various design parameters. The modulation signals such as mQAM, CP-OFDM, FBMC, UF-OFDM have been designed in MATLAB. For the optical transmission and reception, VPItransmissionMaker is used. The received signal is again offline processed using MATLAB for demodulation.

For experimental evaluation, the electro-optical setup is implemented. The offline designed 5G based RF signals (OFDM, FBMC, UF-OFDM) were loaded in the arbitrary waveform generator (AWG) for generating 5G RF signals. To generate mm-wave carrier, two Mach-Zehnder modulators (MZM) based method as well as a photo-mixing method are utilized. In the two MZM method, the 5G signal is carried optically by a free running laser with an MZM operating at linear transmission point and converted to mm-wave by another MZM operated at minimum transmission point driven by half of the desired mm-wave carrier frequency. In the photomixing method, the RF signal is carried optically by externally modulating a free running laser and converted to mm-wave by photomixing with another free running laser at a frequency offset of mm-wave frequency. The received mm-wave signals were down converted to baseband and digital signal processing routines were developed in MATLAB for the demodulation. The system performance is evaluated with bit error rate (BER) and error vector magnitude (EVM) measurements.

3. New scientific results: Theses

I thesis:

To achieve the 5G deployment goal with RoF technology, the realization of high SNR of the received signal and support of higher order vector modulation formats are important issues. The maximization of the SNR in OSSB scheme can be achieved by OVSF scheme. OVSF scheme enhances the strength of the received signal as well as balances the intensities of the generated harmonic components to minimize the distortion, which improves the system performance. In this thesis, I proposed the OVSF scheme for improving SNR in RoF system. I applied alternative technique of cascaded modulators to generate OVSF scheme and evaluated the performance of this scheme with the conventional schemes.

To analyze the proposed OVSF scheme, I used the series Mach Zehnder modulator (MZM) and phase modulator (PM) configuration based sideband generation method as shown in Fig. 1. In this method, firstly ODSB can be generated by using MZM. The MZM can be operated in a linear region of the MZM transfer curve and only PM index can be tuned for generating OVSF scheme. By tuning the PM index, each first order sideband's intensities can be controlled independent to each other and undesired

harmonics intensity can be minimized. The signal power can be increased through the use of partially suppressed upper side band (USB) or lower side band (LSB) and the harmonic distortion can be reduced by reducing the harmonics power, these cause improvement in SNR. These effects can be realized by properly tuning the PM index. The choice of the proper modulation parameters can minimize the CD effect as well as enhances the SNR. The required PM index for maximum SNR depends on the used frequency and fiber length. The SNR depends not only on the received signal power but also on the harmonic distortion of the RoF system.

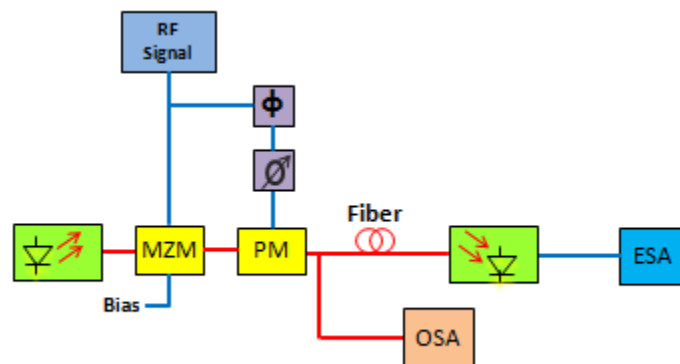


Fig. 1 The functional block diagram for generation and performance analysis of the proposed OVSB scheme with OSSB scheme. OSA= optical spectrum analyzer, ESA: electrical signal analyzer.

Some slightly complex methods have been reported in the literature for achieving the SNR optimization goal [16, 17 and 19]. These methods include; dual electrode Mach Zehnder modulator (DMZM) with tunable optical filter, using polarization modulators, optical injection locked laser based technique etc. The optical injection locked laser based technique requires precise measurements and two lasers. The presented OVSB scheme generated from the simple series MZM and PM configuration does not require a tunable optical filter to suppress the sideband, it also does not require an additional optical amplifier because the total optical power remains constant. Since the proposed configuration does not require an additional optical tunable filter, the problems of a tunable filter method like filter instability and precise frequency tuning are avoided. Also, PM does not require a bias voltage, so it is less affected by the environmental fluctuations.

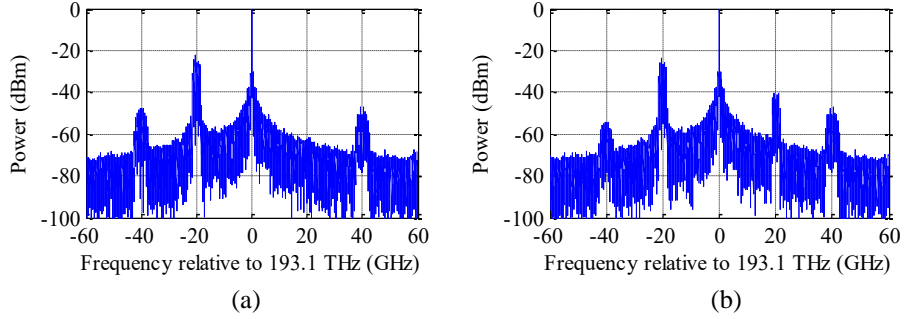


Fig. 2 (a). Optical spectrum for OSSB scheme at 20 GHz, the sideband at 20 GHz has been completely suppressed leaving behind -20 GHz sideband. The sidebands at ± 40 GHz are undesired harmonics. **(b)** Optical spectrum for OVSB scheme at 20 GHz, the sideband at +20 GHz has been partially suppressed. The sidebands at ± 40 GHz are undesired harmonics in which the USB power level is higher than the LSB. Also the harmonics' power levels are lower than in the case of OSSB scheme

Thesis 1.1: Analytical description

In the following discussions, I provide the analytical expression of proposed series MZM and PM configuration for the generation of OSSB and OVSB schemes.

Let $E_{in}(t) = A_c \exp(j\omega_c t)$ be an optical carrier and $M(t) = \cos(\omega_d t)$ a modulation electrical signal where ω_c and ω_d denote the frequency of the optical carrier and electrical signal, respectively. The general expression for the output electric field from the MZM can be given as [20]

$$E_{out1}(t) = \frac{A_c}{2} \left[\exp\left(\frac{j\pi M(t)}{V_\pi}\right) + \exp\left(\frac{j\pi V_b}{V_\pi}\right) \right] E_{in}(t) \quad (1)$$

where V_π is the half wave voltage of the modulator and V_b is the applied dc bias to the modulator. Next we denote $m = \frac{\pi M(t)}{V_\pi}$ the phase modulation index for MZM and $c = \frac{\pi V_b}{V_\pi}$ the constant phase shift to the MZM. Now simplifying the above equation yields

$$E_{out1}(t) = A_c \{ \cos(c) \cdot \cos[m \cdot \cos(\omega_d t)] - \sin(c) \cdot \sin[m \cdot \cos(\omega_d t)] \} E_{in}(t) \quad (2)$$

Equation (2) can be simplified further using Bessel formulae. Let $p = A_c \cdot \cos(c) \cdot J_0(m)$ and $q = A_c \cdot \sin(c) \cdot J_1(m)$ for the calculation convenience where J_x , $x = 0, 1, \dots$ are the coefficients of the Bessel function of the first kind. Taking only the first order sidebands, the above equation will be reduced to

$$E_{out1}(t) = E_{in}(t) [p + q \cdot (e^{j\omega_d t} + e^{-j\omega_d t})] \quad (3)$$

In equation (3), we neglected the higher order sidebands by assuming the very low power associated with them considering the case of small signal analysis. Let us suppose that $\sin(\omega_d t)$ is the PM driving signal. When MZM and PM are connected the field output from PM can be written as

$$E_{out2}(t) = E_{in2}(t) e^{j[\theta \cdot \sin(\omega_d t)]} \quad (4)$$

where \varnothing is the phase modulation index in radians. The term $E_{in2}(t)$ is equal to $E_{out1}(t)$. Now simplifying the second term in equation (4) using Bessel formulae and taking only the first order sidebands yields

$$E_{out2}(t) = E_{in2}(t)[J_0(\varnothing) + J_1(\varnothing)(e^{j\omega_d t} - e^{-j\omega_d t})]. \quad (5)$$

After simplification and neglecting the higher frequency terms above equation will be reduced to

$$\frac{E_{out2}(t)}{E_{in}(t)} = p \cdot J_0(\varnothing) + (q \cdot J_0(\varnothing) + p \cdot J_1(\varnothing)) e^{j\omega_d t} + (q \cdot J_0(\varnothing) - p \cdot J_1(\varnothing)) e^{-j\omega_d t} . \quad (6)$$

In above equation, the first term is optical carrier, the second term is USB and the third term is LSB.

The nonlinear transfer characteristic of the modulator causes the creation of an infinite number of sidebands. Among these, second and third order sidebands are considered significant for harmonic distortion. Fig. 3 shows the fundamental (ω_d), second ($2\omega_d$), and third ($3\omega_d$) order harmonics' power variations with fiber lengths for single MZM and for series MZM and PM cases for 20 GHz RF signal. The fiber attenuation was not considered for these simulations to observe the harmonics' power variations due to CD.

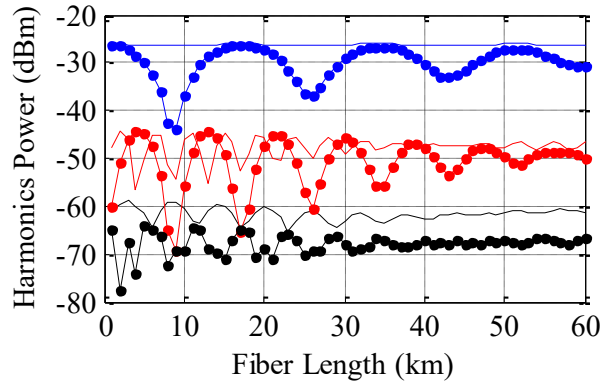


Fig. 3. Harmonic powers. Colours- blue: fundamental, red: second order, black: third order. Lines- with(.): MZM, solid plain: series MZM and PM.

In this thesis, I proposed the series MZM and PM configuration to enhance the SNR in RoF system. I provided the analytical expression of series MZM and PM configuration for the generation of OSSB and OVSF schemes. Based on the theoretical analysis I proved that USB based OSSB can be generated in the condition $q \cdot J_0(\varnothing) = p \cdot J_1(\varnothing)$ and LSB based OSSB scheme can be produced in the condition $q \cdot J_0(\varnothing) = -p \cdot J_1(\varnothing)$. I demonstrated that the proposed configuration is suitable for OVSF generation, which is obtained with unequal sideband intensity. To achieve this, I introduced a new scaling parameter $k = \pm \frac{q \cdot J_0(\varnothing)}{p \cdot J_1(\varnothing)}$, which determines the extent of the sideband suppression. For maximum suppression its value

will be 1 which leads to the OSSB scheme and for partial suppression its value can be considered less than 1 resulting in the OVSB scheme.

Also, I studied the behavior of the harmonics' power for MZM and series MZM and PM for various fiber lengths by numerical simulations. I demonstrated that, second order harmonics is a major harmonic distortion contributor in the single MZM case. Third order harmonic has a higher level of power in the proposed series MZM and PM configuration compared to single MZM case. However still second order distortion dominates in the system.

Thesis 1.2: Comparisons of OVSB scheme with conventional schemes

The received signal power for the various modulation schemes with respect to the frequency is given in Fig. 4, which shows that OVSB scheme improves the received signal power. With the proposed method, the power of the generated OSSB and OVSB signals are higher than ODSB. If the optical tunable filter is used to suppress one of the sideband for generating OVSB scheme the total optical power is decreased due to the insertion loss as well as due to the sideband power suppression. But, the proposed method is flexible that by tuning the PM index only, the desired sideband power suppression can be achieved and the total optical power remains constant.

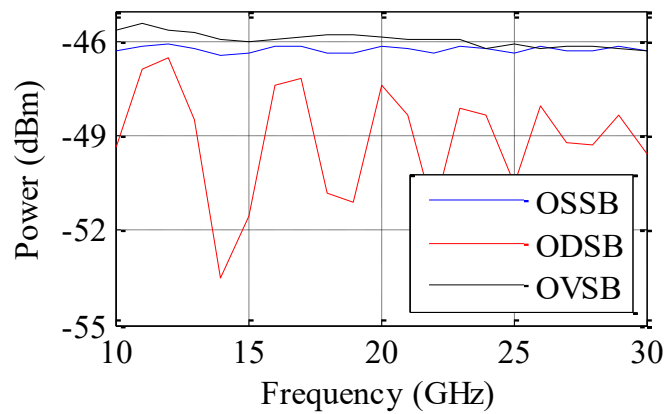


Fig. 4. Received signal power for various sideband modulation schemes for different frequencies after 50 km fiber length.

I investigated the optimum parameters for OSSB and OVSB schemes and compared the symbol error rate (SER) performance for the 4QAM signal through numerical simulation as shown in Fig. 5.

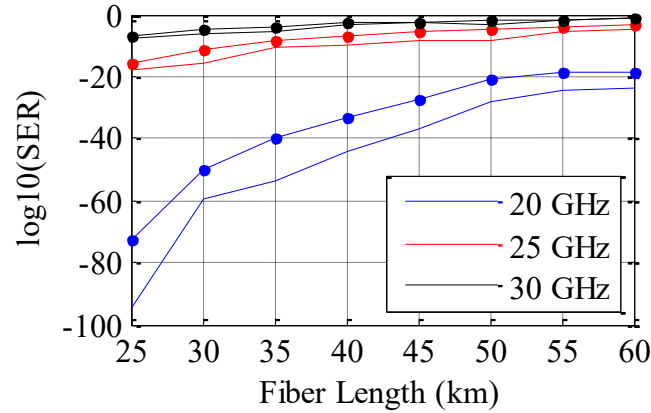


Fig. 5. SER performance of OSSB and OVSB schemes for different frequencies and fiber lengths for 5 Gbps, 4QAM modulation format signal. The curves with (.) are for OSSB scheme and solid plain curves are for OVSB scheme. The SER were estimated using Gaussian estimation method.

The summary of each sideband modulation scheme which can be generated with the proposed method is given in Table 1.

TABLE 1 COMPARISON OF DIFFERENT MODULATION SCHEMES

Modulation Schemes	Generation Methods	CD effect	Received signal SNR	Application
ODSB	MZM, PM MZM + PM	High	Low (varies periodically)	Short distance, low RF
OCS-DSB	MZM, PM, MZM + PM, MZM + filter	Low	High	Long distance/ high RF, no vector signal
OSSB	MZM + filter, PM + filter, MZM + PM	Low	Low	Moderate distance, high RF
OVSB	MZM + filter, PM + filter, MZM + PM	Moderate	High	Long distance, high RF

In this thesis, I showed that the performance of OVSB scheme in RoF system is better than the OSSB scheme if proper PM index is selected.

Also, I showed that the series MZM and PM configuration is flexible method to generate various modulation schemes. Although the power of the desired sideband and undesired harmonics can be changed, the total power remains constant. Therefore, the proposed method doesn't require an additional optical amplifier and doesn't require an optical filter to suppress sideband power. One can flexibly change between ODSB, OSSB and OVSB schemes just tuning the PM index and without the use of optical filter, which is very important for future software defined radio.

Related own publications: J3, C3, C4 and C5.

II thesis:

FBMC modulation format is considered as a potential candidate for future wireless 5G due to its feature of high suppression for out-of-band emissions, which allows combining multiple sub-bands with very narrow band-gaps, and hence increasing the overall of the wireless transmission capacity. In this thesis, I designed the multi-sub-bands FBMC signal and experimentally demonstrated the high bit rate signal transmission of multi sub-bands FBMC signals at mm-wave for RoF system. Also, I demonstrated through numerical simulation, the performance of the wired-wireless converged PON using 4-PAM as a wired signal and FBMC as a wireless signal.

Thesis 2.1: high bit rate multi-sub-bands FBMC transmission in mm-wave RoF system

The performance comparison of OFDM and FBMC carrier aggregated signals at mm-wave frequencies was recently studied with the aggregated bandwidth of less than 1.5 GHz [21, 22]. These demonstrations show that the FBMC outperforms the OFDM for equivalent design parameters. Adaptively modulated FBMC was also demonstrated in the wired-wireless converged network with the aggregated bandwidth of 1.5 GHz [23]. All of the above- mentioned demonstrations of FBMC based multiple sub-band signals for mm-wave transmission are dealt with sub-band bandwidth of less than 220 MHz and the aggregate bandwidth of less than 1.5 GHz, and hence low overall data rate.

In this thesis, the designed multi sub-bands FBMC system consists of 5 sub-bands of 800 MHz with an inter sub-band gaps of 781.25 kHz as shown in Fig. 6. The composite 5 sub-bands FBMC signal is generated with no band-gap between dc to the first sub-band to preserve the bandwidth of the system. Each FBMC sub-band consists of 1024 sub-carriers and is modulated with uncorrelated data sequences. The offline coded RF multi-sub-bands FBMC signal is loaded to the AWG for the generation. The designed experimental setup is given in Fig. 7. The aggregate FBMC signal is carried optically by externally modulating a free running laser and converted to mm-wave by photomixing with another free running laser at a frequency offset of 53 GHz. At the receiver, the received electrical mm-wave signal is down-converted to an intermediate frequency (IF) and then post-processed using digital signal processing (DSP) techniques. With the use of the simple recursive least square (RLS) equalizer in the DSP receiver, the achieved aggregate data rate is 8 Gbps and 12 Gbps for 16 quadrature amplitude modulation (QAM), and 64 QAM, respectively with a total bandwidth of 4.2 GHz.

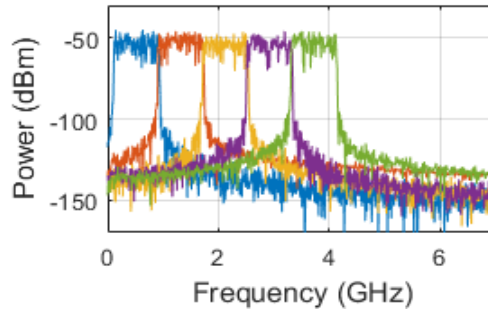


Fig. 6. Electrical spectrum of offline generated 5 sub-bands FBMC signal.

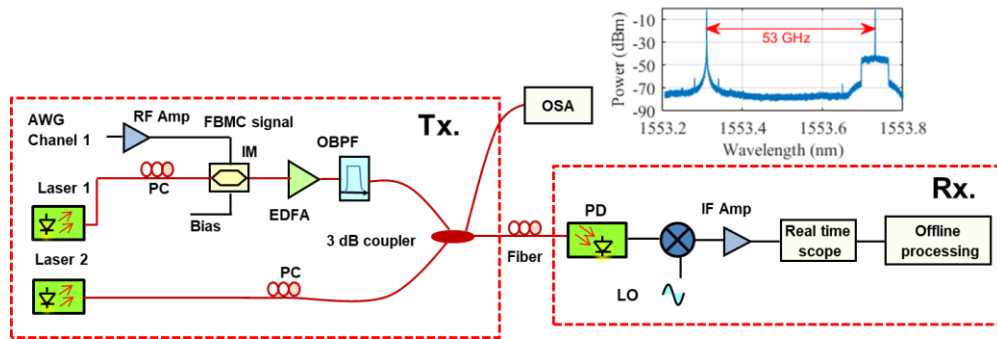


Fig. 7. Experimental setup for multi FBMC sub-bands transmitter and receiver. The inset figure is the optical spectrum of the mixed optical signals at the optical spectrum analyzer (OSA).

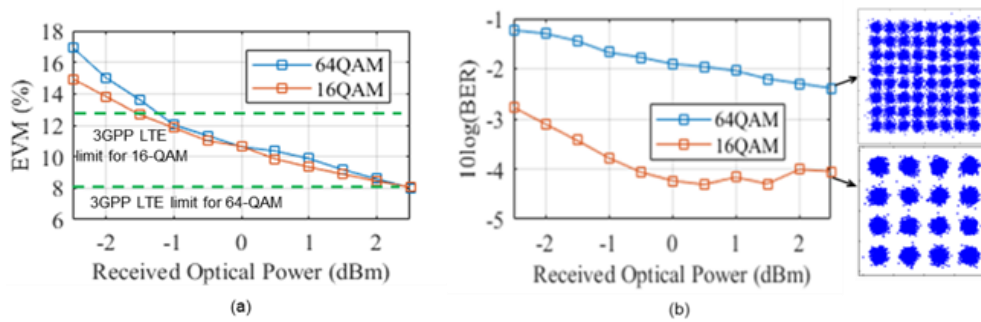


Fig. 8. (a) EVM and (b) BER performances versus ROP for 5 sub-bands FBMC signal. Inset figures are the constellations of 16QAM and 64QAM for ROP of 2.5 dBm.

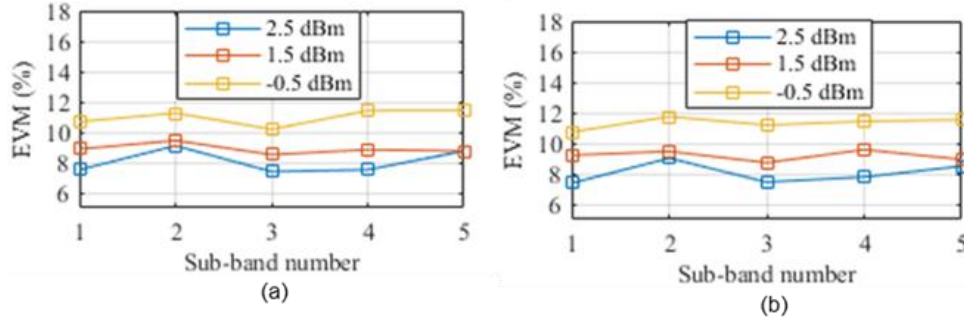


Fig. 9. EVM performances of each sub-band FBMC signal for (a) 16 QAM (b) 64 QAM.

This experiment achieved EVM below 12.5 % for 16 QAM and 8% for 64 QAM as a figure of merit as proposed by 3GPP LTE [24] as shown in Fig. 8(a). These limits were achieved for the received optical power of -1.5 dBm and 2.5 dBm for 16 QAM and 64 QAM, respectively. The BER values of 8×10^{-5} for 8 Gbps case using 16 QAM and 4×10^{-3} for 12 Gbps case using 64QAM are achieved for the received optical power of 2.5 dBm as shown in Fig. 8(b). The individual sub-bands EVM percentages are also given in Fig. 9.

In this thesis, I experimentally demonstrated the transmission of high bit rate multi-sub-bands FBMC RF signal in mm-wave RoF system. The demonstrated results satisfied standard 3GPP LTE EVM percentage limit as well as forward error correction (FEC) limit. The demonstrated data rates are the highest data rate achieved so far found in the literature for mm-wave RoF systems. Due to the high suppression of out-of-band emission, I believe that the multiplexed FBMC sub-bands will meet the expectation for the future 5G wireless with high data rate transmission for multi-user, and multi-bands wireless services feasibility.

Thesis 2.2: Wired-wireless converged PON using 4-PAM and FBMC

Future 5G based PON are expected as capable of a simultaneous provision of wired and wireless services for multi-users. The PON provides the high capacity and flexibility in signal delivery through the fixed access network. PON is considered as an effective solution for 5G based wireless signals backhauling and fronthauling [25-29]. The future 5G systems should be capable of supporting multi-services/signals to keep the compatibility with the current legacy wired/wireless services. In this regard, it is important to study and analyze the convergence and delivery of potential 5G wireless signals with wired signals in the future PON systems.

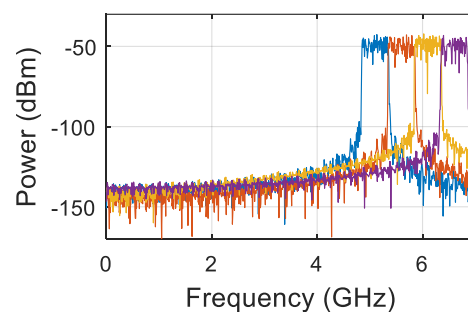
In the designed system, the multiplexed wired 4-PAM and wireless multi-sub-bands FBMC signal is generated and transmitted with simple intensity modulation in optical line terminal (OLT). In the optical

network unit (ONU) the wired and wireless signal from received converged signal is extracted using an electrical square band-pass filter and separately demodulated using DSP techniques.

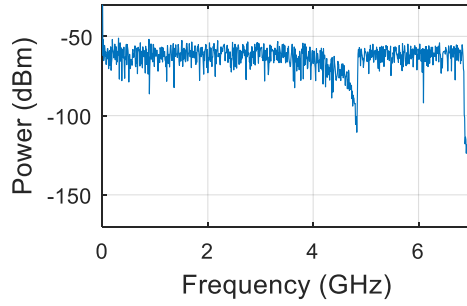
The 4-PAM modulation format can be used in cost-efficient intensity modulation direct detection (IM/DD) systems and it provides the double bandwidth efficiency compared to conventional on-off keying (OOK) modulation format. Due to these benefits, recently huge research interests are shown on this modulation format for cost-effective optical access network design [30-32].

OFDM and FBMC based PON was experimentally demonstrated in [33]. Recently, the convergence of potential 5G modulation formats such as universal filter multi-carrier (UFDM) and generalized filter multi-carrier (GFDM) as wireless signals and 4-PAM signal as a wired signal in a PON has been demonstrated [34]. This demonstration deals with the single sub-band UFDM and GFDM modulation formats with a very low bandwidth of 1.95 MHz for each modulation format.

All of the above mentioned recent demonstrations of wired/wireless convergence in PON have not been dealt with the convergence of multi-sub-bands FBMC as a wireless and 4-PAM as a wired signal. In this thesis, I demonstrated the convergence of 4 sub-bands FBMC as a wireless signal and 4-PAM as a wired signal in a PON. The bandwidth of the designed 4-PAM baseband signal is 4.8 GHz. The aggregate bandwidth of the designed 4 sub-bands FBMC signal is 2.0015 GHz with inter-sub-band gap frequency of 488.28 kHz as shown in Fig. 10(a). The multiplexed composite signal spectrum is given in Fig. 10(b). The aggregate data rate with 16QAM modulation order for 4-sub-bands FBMC is 4 Gbps and 4-PAM is 8 Gbps. The implemented system setup is given in Fig. 11. The system setup was designed in VPItransmissionMaker simulator with MATLAB co-simulation. The 4-PAM and FBMC sub-bands are extracted and demodulated in the receiver by using DSP techniques. I evaluated the performance of the converged signals by simulating various design parameters using BER calculations.



(a)



(b)

Fig. 10. Offline generated spectra of (a) 4 sub-bands FBMC (b) multiplexed 4-PAM and 4 sub-bands FBMC signal.

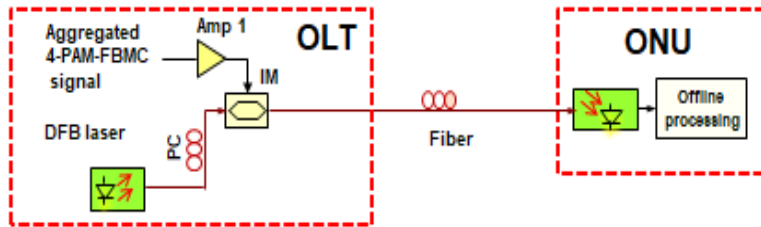


Fig. 11. Block diagram of PON setup with OLT and ONU.

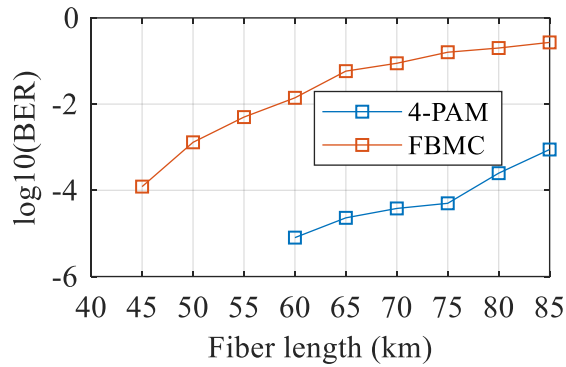


Fig. 12. Numerical simulation results of BER versus fiber length performances for 4-PAM and 4 sub-bands FBMC signals.

The BER with respect to fiber length is given in Fig. 12. This investigation showed, with the very low-performance degradation ($BER < 10^{-6}$) the converged signal can be transmitted for the distance up to 40 km for the received optical power (ROP) of -4.1 dBm with the laser linewidth of 10 MHz. The BER of 10^{-3} can be obtained at ROP of -22 dBm for the case of 4 sub-bands FBMC and -21 dBm for the case of 4-PAM at 40 km fiber length and laser linewidth of 10 MHz. The FBMC shows better performance compared to 4-PAM for separate transmission.

In this thesis, for the first time; I proposed and demonstrated by numerical simulation the simultaneous delivery of wired 4-PAM and wireless multi-sub-bands FBMC signals in one wavelength using one laser source for the future 5G PON. The converged signal can be transmitted with BER of less than standard FEC limit for the few tens of km. I showed by simulation that, FBMC is more affected by the laser linewidth and the interference effect compared to 4-PAM in the converged signal transmission scenario. Also, due to the double bandwidth efficiency of the 4-PAM, it will be attractive candidate compared to conventional OOK in baseband signal transmission scenario.

Related own publications: J2, J4, C2.

III thesis:

UF-OFDM modulation format is considered as a potential candidate for future wireless 5G due to its features of better spectral efficiency and lower spectral side lobes compared to the cyclic prefix OFDM (CP-OFDM). In this thesis, I designed the UF-OFDM signal and experimentally demonstrated the generation of the UF-OFDM signal for 5G mm-wave RoF system. In this thesis, I also showed experimentally the wired-wireless converged signal performance in a PON using FBMC and UF-OFDM as a wireless signal and 4-PAM as a wired signal.

Thesis 3.1: UF-OFDM transmission in mm-wave RoF system

Recently, UF-OFDM based RoF system at mm-wave is demonstrated using optical heterodyning technique [35, 36]. In these demonstrations, the heterodyning at 60 GHz has been achieved using laser comb source. Also, the bit rate of 4.56 Gbps has been achieved with 5 sub-bands multiplexed system with band-gap of 15 MHz between each sub-band. In this thesis, for the experimental demonstration of UF-OFDM transmission in 60 GHz, the concatenated MZM based technique is employed as shown in Fig. 13.

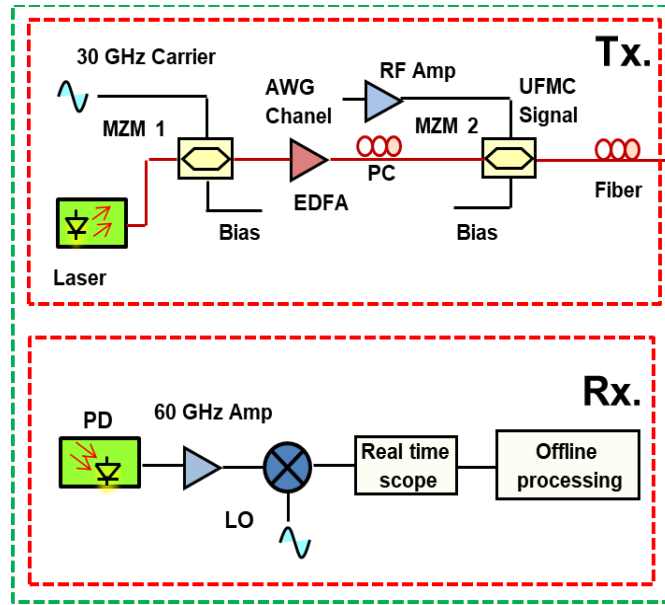


Fig. 13. Experimental setup of transmitter and receiver.

The UF-OFDM signal with 1.25 GHz bandwidth is designed in MATLAB with 400 MHz bandgap between dc to the UF-OFDM signal to avoid the signal to signal beating interference (SSBI) [37]. The offline coded RF UF-OFDM signal is loaded to the AWG for the generation. The UF-OFDM signal is carried optically by a free running laser with an MZM operating at linear transmission point and converted to mm-wave at 60 GHz by another MZM operated at minimum transmission point driven by a 30 GHz electrical carrier. At the receiver, the received electrical mm-wave signal is down-converted to an intermediate frequency (IF) and then post-processed using DSP techniques. The data rate of 3.2 Gbps is achieved with 16 QAM modulation order. The optimum modulation point is determined by varying the driving UF-OFDM signal power to the modulator. The performance is optimized with the use of RLS equalizer. Fig. 14 shows the BER values with respect to the driving signal power. The BER value of 10^{-3} is achieved satisfying the standard FEC limit for the driving RF signal power of 3 dBm.

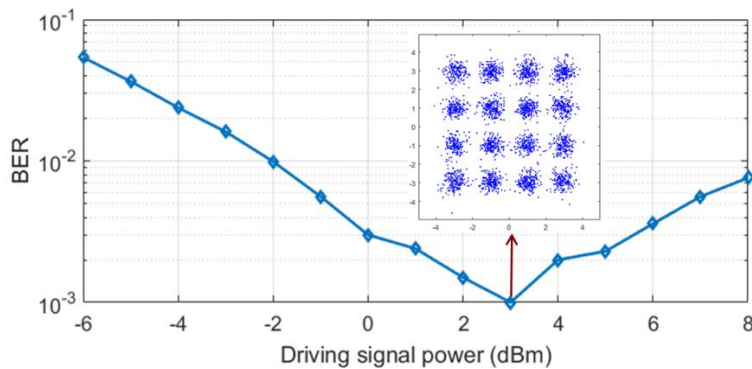


Fig. 14. Measurement results of BER versus driving signal power.

In this thesis, I experimentally demonstrated the potential 5G modulation format UF-OFDM transmission at 60 GHz in a RoF system by employing two MZMs. The measurement results satisfied the standard FEC limit. I proved that, due to the high suppression of out-of-band emission and better spectral efficiency, the UF-OFDM signal will meet the expectation for the future 5G wireless with high data rate transmission.

Thesis 3.2: Wired-wireless converged PON using 4-PAM, FBMC and UF-OFDM

In this thesis, I experimentally demonstrated the simultaneous delivery of wired and wireless signals in a PON. The concept of the composite multiplexed signal generation is given in Fig. 15 and experimental setup is given in Fig. 16. The offline coded multiplexed wired 4-PAM and wireless FBMC and UF-OFDM signal is loaded to the AWG for the generation. Thus obtained signal is transmitted with intensity modulation in the OLT. The received signal spectrum in ONU is given in Fig. 17. In the ONU, the wired and wireless signals from the received composite signal are extracted using an electrical square band-pass filter and separately demodulated using DSP techniques. In this work, by using FBMC signal of 1 GHz, UF-OFDM of 500 MHz and 4-PAM of 1 GHz I demonstrated the performance of converged wired-wireless signal transmission in the PON. Each modulation formats have the bit rate of 2 Gbps and the composite signal bit rate is 6 Gbps. The narrow-band gap of 300 MHz is used to separate the 4-PAM and FBMC and 150 MHz is used to separate the FBMC and UF-OFDM. The BER and EVM values have been measured after 25 km fiber length for the performance analysis.

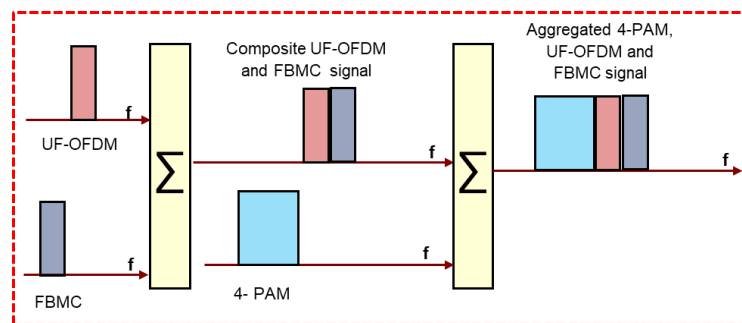


Fig. 15. 4-PAM, FBMC and UF-OFDM signals multiplexing.

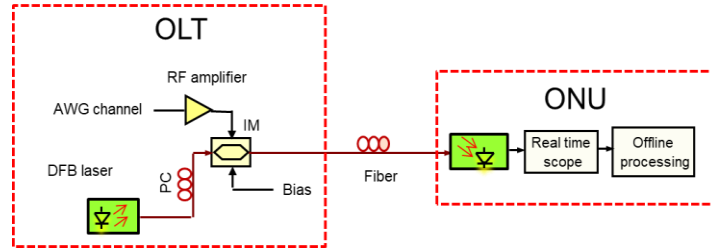


Fig. 16. Block diagram of the PON setup with OLT and ONU.

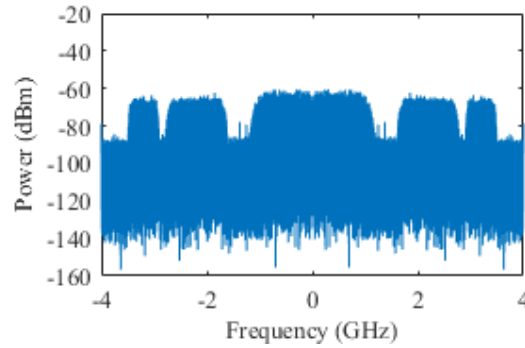


Fig. 17. Spectrum of the received signal (after photodetector) in the ONU, after 25 km fiber length.

As shown in Fig. 18(a), in the converged signal transmission scenario, the BER of 10^{-3} is obtained at the ROP of -11 dBm for FBMC, at -9 dBm for UF-OFDM and at -8 dBm for 4-PAM at 25 km fiber length between OLT and ONU. As shown in Fig. 18(b), the 3GPP EVM (%) limit of 12.5 % is achieved at the ROP of -9 dBm and -5 dBm for the 16-QAM FBMC and 16-QAM UF-OFDM respectively.

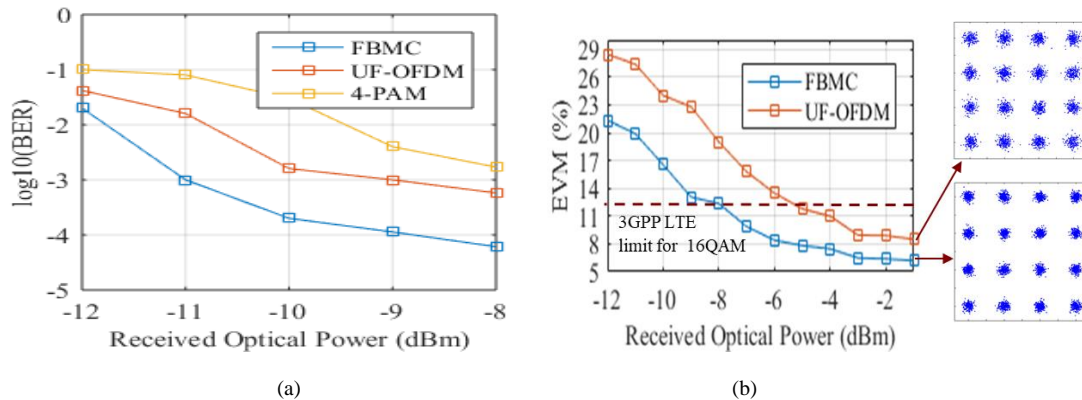


Fig. 18. comparisons for the multiplexed 4-PAM, UF-OFDM and FBMC transmission after 25 km fiber length.

The presented results are achieved with the addition of the simple RLS based post-equalizer in the receiver DSP for the FBMC and UF-OFDM performance optimization. Similarly, for 4-PAM, linear feed forward equalizer (FFE) is used. CD and attenuation are the major impairments for transmitting a wireless

signal through the fiber. The first null power point of the 5 GHz RF signal, with 18 ps/nm/km dispersion and 1551.82 nm laser wavelength occurs at 139 km. In the designed signal, aggregate signal bandwidth from dc is 3.65 GHz and used fiber length is 25 km, thus the power fading effect in the received signal can be considered negligible. In this case, the major transmission impairments are fiber attenuation and electronics noise.

In this thesis, for the first time, I experimentally demonstrated the simultaneous delivery of wired 4-PAM and wireless FBMC and UF-OFDM signals in one wavelength using one laser source for the 5G based PON. I showed that the converged signals can be transmitted by satisfying standard 3GPP EVM percentage limit as well as standard FEC limit for few tens of km. I showed that, for the equivalent design parameters, the FBMC shows better performance compared to 4-PAM and UF-OFDM in both cases; separate transmission and composite transmission. This demonstration proved the feasibility of simultaneous transmission of different signals in 5G network which will be useful for multi-users and multi-service applications.

Related own publications: J1, C1

4. Outlook

In this thesis, I presented the new technique of SNR improvement in RoF system using OVSB scheme. This technique will be effective if there is a fixed fiber length and frequency. For varying fiber length and frequency PM index parameter has to be tuned properly to achieve maximum SNR.

In this thesis, I presented the transmission and performance analysis of the potential 5G based modulation formats such as FBMC and UF-OFDM for mm-wave RoF system. The presented results are achieved without the use of the analog envelope detector to down-convert the mm-wave frequency to a baseband signal. I used a mixer, an RF amplifier and broadband amplifier which add extra electronics noise to the signal that reduces the SNR of the received signal. SNR can be improved by employing the analog envelope detector instead of LO and mixer. The amplifiers with better flatness in the frequency response can improve the results. The presented results are for without wireless channel transmission. It would be interesting to analyze the performance by adding the wireless transmission after the photodetector using antennas.

I also presented the 4-PAM as a wired and FBMC and UF-OFDM as a wireless multiplexed signal transmission for 5G PON. Very interesting results are achieved. These experiments can be extended to optimize the various system design parameters such as gap frequency between signals, maximum

achievable bit rate, bandwidth, fiber length etc. The results presented in this thesis will be quite useful for mobile/wireless companies.

5. Publication related to PhD thesis

Journal Papers

J1. Hum Nath Parajuli, Julien Poette, Robert Horvath, Eszter Udvary, "Wired-Wireless Converged Passive Optical Network Using 4-PAM, FBMC and UF-OFDM", under review in *Journal of Lightwave Technology*.

J2. Hum Nath Parajuli, Shams Haymen, Luis Guerrero Gonzalez, Eszter Udvary, Cyril Renaud, John Mitchell "Experimental demonstration of multi-Gbps multi-sub-bands FBMC transmission in mm-wave radio over fiber system". *Opt. Express* 26, 7306-7312 (2018).

J3. Hum Nath Parajuli, Eszter Udvary, "Novel Vestigial Sideband Modulation Scheme to Enhance the SNR in Radio Over Fiber Systems", *RADIOENGINEERING*, VOL. 26, NO. 4, DECEMBER 2017.

J4. Hum Nath Parajuli, Eszter Udvary, "Wired-Wireless Converged Passive Optical Network Using 4-PAM and FBMC", *Info communication Journal*, 10(2), June 2018.

Conference Papers

C1. Hum Nath Parajuli, J. Poëtte and E. Udvary, "UF-OFDM Based Radio Over Fiber for 5G Millimeter Wave Small Cell Radio Access Network," *2018 11th International Symposium on Communication Systems, Networks & Digital Signal Processing (CSNDSP)*, Budapest, Hungary, 2018, pp. 1-4.

C2. Hum Nath Parajuli, Shams Haymen, Eszter Udvary, "Synchronization and Channel Estimation in Experimental M-QAM OFDM Radio over Fiber Systems Using CAZAC Based Training Preamble", *21st International Conference on Optical Networks Design and Modeling*, May, 2017.

C3. Hum Nath Parajuli, Eszter Udvary, "A Vestigial Sideband Modulation Scheme in Radio Over Fiber System Using Electro-Optic Modulators", in *2016 18th International conference on Transparent Optical Networks (ICTON)*, July, 2016.

C4. Hum Nath Parajuli, Eszter Udvary, "Optimization of Optical Carrier to Sideband Ratio for the concatenated AM-PM Based Optical Single Sideband Radio Over Fiber System", in *2016 21st European Conference on Networks and Optical Communications (NOC)*, June, 2016.

C5. Hum Nath Parajuli, Eszter Udvary, Aron Szabo, "Improving the Capacity of Radio Over Fiber System using Pol-Mux and Vector Signal Transmission" in *5th Mesterproba, National Student Conference*, May 26th, 2016.

Acknowledgement

This thesis work has been carried out within the Marie Curie innovative training network project FiWiN5G (fiber-wireless integrated networks for 5th generation delivery), supported from European Union's Horizon 2020 research and innovation program. The project involves 11 partners in 9 European countries. I mainly worked in the optical and microwave technology laboratory (OMT) of Budapest

University of Technology and Economics. For conducting mm-wave transmission experiments I went to University College London (UCL), London, UK and IMEP-LAHC laboratory, CNRS, Univ. Grenoble Alpes, Grenoble, France. Investigated results were reported in the bi-annual basis to the meeting of the FiWiN5G training network framework. The results were presented and published in various peer review international conferences and international journals.

References

1. Rappaport, T.S.; Shu Sun; Mayzus, R.; Hang Zhao; Azar, Y.; Wang, K.; Wong, G.N.; Schulz, J.K.; Samimi, M.; Gutierrez, F., "Millimeter Wave Mobile Communications for 5G Cellular: It Will Work!," in *Access, IEEE*, vol.1, no., pp.335-349, 2013
2. L. Wei, R. Q. Hu, Y. Qian and G. Wu, "Key elements to enable millimeter wave communications for 5G wireless systems," in *IEEE Wireless Communications*, vol. 21, no. 6, pp. 136-143, December 2014. doi: 10.1109/MWC.2014.7000981.
3. Thomas, V.A.; Ghafoor, S.; El-Hajjar, M.; Hanzo, L., "A Full-Duplex Diversity-Assisted Hybrid Analogue/Digitized Radio Over Fibre for Optical/Wireless Integration," in *Communications Letters, IEEE*, vol.17, no.2, pp.409-412, February 2013
4. D. Novak *et al.*, "Radio-Over-Fiber Technologies for Emerging Wireless Systems," in *IEEE Journal of Quantum Electronics*, vol. 52, no. 1, pp. 1-11, 2016. doi: 10.1109/JQE.2015.2504107.
5. Gee-Kung Chang; Lin Cheng; Mu Xu; Guidotti, D., "Integrated fiber-wireless access architecture for mobile backhaul and fronthaul in 5G wireless data networks," in *Avionics, Fiber-Optics and Photonics Technology Conference (AVFOP), 2014 IEEE*, vol., no., pp.49-50, 11-13 Nov. 2014
6. C. Liu, H. C. Chien, S. H. Fan, J. Yu and G. K. Chang, "Enhanced Vector Signal Transmission Over Double-Sideband Carrier-Suppressed Optical Millimeter-Waves Through a Small LO Feedthrough," in *IEEE Photonics Technology Letters*, vol. 24, no. 3, pp. 173-175, Feb.1, 2012. doi: 10.1109/LPT.2011.2175719
7. B. Hraimel *et al.*, "Optical Single-Sideband Modulation With Tunable Optical Carrier to Sideband Ratio in Radio Over Fiber Systems," in *Journal of Lightwave Technology*, vol. 29, no. 5, pp. 775-781, March1, 2011. doi: 10.1109/JLT.2011.2108261
8. V. A. Thomas, M. El-Hajjar and L. Hanzo, "Performance Improvement and Cost Reduction Techniques for Radio Over Fiber Communications," in *IEEE Communications Surveys & Tutorials*, vol. 17, no. 2, pp. 627-670,2015. doi: 10.1109/COMST.2015.2394911
9. Y. Gao, A. Wen, Y. Chen, S. Xiang, H. Zhang and L. Shang, "An Analog Photonic Link With Compensation of Dispersion-Induced Power Fading," in *IEEE Photonics Technology Letters*, vol. 27, no. 12, pp. 1301-1304, 2015. doi: 10.1109/LPT.2015.2421271
10. J. Y. Sung, C. W. Chow, C. H. Yeh, Y. Liu and G. K. Chang, "Cost-effective mobile backhaul network using existing ODN of PONs for the 5G wireless systems," in *IEEE Photonics Journal*, vol. 7, no. 6, pp. 1-6, Dec. 2015. doi: 10.1109/JPHOT.2015.2497222
11. B. Skubic, M. Fiorani, S. Tombaz, A. Furuskär, J. Mårtensson and P. Monti, "Optical transport solutions for 5G fixed wireless access [Invited]," in *IEEE/OSA Journal of Optical Communications and Networking*, vol. 9, no. 9, pp. D10-D18, Sept.2017. doi:10.1364/JOCN.9.000D10
12. X. Liu and F. Effenberger, "Emerging optical access network technologies for 5G wireless [invited]," in *IEEE/OSA Journal of Optical Communications and Networking*, vol. 8, no. 12, pp. B70-B79,2016. doi:10.1364/JOCN.8.000B70.

13. A. Tzanakaki *et al.*, "Wireless-optical network convergence: enabling the 5G architecture to support operational and end-user services," in *IEEE Communications Magazine*, vol. 55, no. 10, pp. 184-192, OCTOBER 2017. doi: 10.1109/MCOM.2017.1600643.
14. B. Skubic, M. Fiorani, S. Tombaz, A. Furuskär, J. Mårtensson and P. Monti, "Optical transport solutions for 5G fixed wireless access [Invited]," in *IEEE/OSA Journal of Optical Communications and Networking*, vol. 9, no. 9, pp. D10-D18, Sept. 2017. doi: 10.1364/JOCN.9.000D10.
15. C. Browning *et al.*, "5G wireless and wired convergence in a passive optical network using UF-OFDM and GFDM," *2017 IEEE International Conference on Communications Workshops (ICCWorkshops)*, 2017, pp. 386-392. doi:10.1109/ICCW.2017.7962688.
16. Y. Gao, A. Wen, Z. Peng and Z. Tu, "Analog Photonic Link With Tunable Optical Carrier to Sideband Ratio and Balanced Detection," in *IEEE Photonics Journal*, vol. 9, no. 2, pp. 1-10, April 2017. doi: 10.1109/JPHOT.2017.2667891
17. B. Hraimel *et al.*, "Optical Single-Sideband Modulation With Tunable Optical Carrier to Sideband Ratio in Radio Over Fiber Systems," in *Journal of Lightwave Technology*, vol. 29, no. 5, pp. 775-781, March 1, 2011. doi: 10.1109/JLT.2011.2108261
18. Javier S, S. Fandino *et. al.*, A monolithic integrated photonic microwave filter. *Nature Photonics* .2016. DOI: 10. 1038 /nphoton .2016.233.
19. J. Xiong *et al.*, "A Novel Approach to Realizing SSB Modulation With Optimum Optical Carrier to Sideband Ratio," in *IEEE Photonics Technology Letters*, vol. 25, no. 12, pp. 1114-1117, June 15, 2013. doi: 10.1109/LPT.2013.2260141
20. V. A. Thomas, M. El-Hajjar and L. Hanzo, "Millimeter-Wave Radio Over Fiber Optical Upconversion Techniques Relying on Link Nonlinearity," in *IEEE Communications Surveys & Tutorials*, vol. 18, no. 1, pp. 29-53, 2016. doi: 10.1109/COMST.2015.2409154
21. J. Zhang *et al.*, "Full-Duplex Quasi-Gapless Carrier Aggregation Using FBMC in Centralized Radio-Over-Fiber Heterogeneous Networks," in *Journal of Lightwave Technology*, vol. 35, no. 4, pp. 989-996, Feb. 15, 2017. doi: 10.1109/JLT.2016.2608138
22. M. Xu *et al.*, "FBMC in Next-Generation Mobile Fronthaul Networks With Centralized Pre-Equalization," in *IEEE Photonics Technology Letters*, vol. 28, no. 18, pp. 1912-1915, Sept. 15, 2016. doi: 10.1109/LPT.2016.2575060
23. S. Y. Jung, S. M. Jung and S. K. Han, "AMO-FBMC for Asynchronous Heterogeneous Signal Integrated Optical Transmission," in *IEEE Photonics Technology Letters*, vol. 27, no. 2, pp. 133-136, Jan. 15, 2015. doi: 10.1109/LPT.2014.2363197
24. ETSI, "LTE; Evolved universal terrestrial radio access (E-UTRA); Base station (BS) radio transmission and reception", 2015.
25. J. Y. Sung, C. W. Chow, C. H. Yeh, Y. Liu and G. K. Chang, "Cost-effective mobile backhaul network using existing ODN of PONs for the 5G wireless systems," in *IEEE Photonics Journal*, vol. 7, no. 6, pp. 1-6, Dec. 2015. doi: 10.1109/JPHOT.2015.2497222
26. B. Skubic, M. Fiorani, S. Tombaz, A. Furuskär, J. Mårtensson and P. Monti, "Optical transport solutions for 5G fixed wireless access [Invited]," in *IEEE/OSA Journal of Optical Communications and Networking*, vol. 9, no. 9, pp. D10-D18, Sept. 2017. doi:10.1364/JOCN.9.000D10

27. X. Liu and F. Effenberger, "Emerging optical access network technologies for 5G wireless [invited]," in *IEEE/OSA Journal of Optical Communications and Networking*, vol. 8, no. 12, pp. B70-B79, 2016. doi:10.1364/JOCN.8.000B70.
28. A. Tzanakaki *et al.*, "Wireless-optical network convergence: enabling the 5G architecture to support operational and end-user services," in *IEEE Communications Magazine*, vol. 55, no. 10, pp. 184-192, OCTOBER 2017. doi: 10.1109/MCOM.2017.1600643.
29. B. Skubic, M. Fiorani, S. Tombaz, A. Furuskär, J. Mårtensson and P. Monti, "Optical transport solutions for 5G fixed wireless access [Invited]," in *IEEE/OSA Journal of Optical Communications and Networking*, vol. 9, no. 9, pp. D10-D18, Sept. 2017. doi: 10.1364/JOCN.9.000D10.
30. I. Lazarou, S. Dris, P. Bakopoulos, B. Schrenk and H. Avramopoulos, "Full-duplex 4-PAM transmission for capacity upgrade in loop-back PONs," in *IEEE Photonics Technology Letters*, vol. 25, no. 12, pp. 1125-1128, June 15, 2013. doi: 10.1109/LPT.2013.2260533.
31. H. K. Shim, H. Kim and Y. C. Chung, "20-Gb/s polar RZ 4-PAM transmission over 20-km SSMF using RSOA and direct detection," in *IEEE Photonics Technology Letters*, vol. 27, no. 10, pp. 1116-1119, May 15, 2015. doi: 10.1109/LPT.2015.2408376.
32. C. Stamatiadis, R. Matsumoto, Y. Yoshida, A. Agata, A. Maruta and K. I. Kitayama, "Full-duplex RSOA-based PONs using 4-PAM with pre-equalization," in *IEEE Photonics Technology Letters*, vol. 27, no. 1, pp. 73-76, Jan.1, 2015. doi: 10.1109/LPT.2014.2361922.
33. A. Saljoghei, F. A. Gutiérrez, P. Perry, D. Venkitesh, R. D. Koipillai and L. P. Barry, "Experimental Comparison of FBMC and OFDM for Multiple Access Uplink PON," in *Journal of Lightwave Technology*, vol. 35, no. 9, pp. 1595-1604, May 1, 2017. doi: 10.1109/JLT.2017.2654319
34. C. Browning *et al.*, "5G wireless and wired convergence in a passive optical network using UF-OFDM and GFDM," *2017 IEEE International Conference on Communications Workshops (ICC Workshops)*, 2017, pp. 386-392. doi:10.1109/ICCW.2017.7962688.
35. C. Browning, E. P. Martin, A. Farhang and L. P. Barry, "60 GHz 5G Radio-Over-Fiber Using UF-OFDM With Optical Heterodyning," in *IEEE Photonics Technology Letters*, vol. 29, no. 23, pp. 2059-2062, Dec. 1, 2017. doi:10.1109/LPT.2017.2763680
36. E. Martin *et al.*, "28 GHz 5G radio over fibre using UF-OFDM with optical heterodyning," *2017 International Topical Meeting on Microwave Photonics (MWP)*, Beijing, 2017, pp. 1-4. doi: 10.1109/MWP.2017.8168651
37. Z. Li *et al.*, "SSBI Mitigation and the Kramers–Kronig Scheme in Single-Sideband Direct-Detection Transmission With Receiver-Based Electronic Dispersion Compensation," in *Journal of Lightwave Technology*, vol. 35, no. 10, pp. 1887-1893, May 15, 2017. doi: 10.1109/JLT.2017.2684298